Editors' Suggestion

High-precision mass measurement of ^{103}Sn restores smoothness of the mass surface

C. M. Ireland,[1,2,*] F. M. Maier,[1] G. Bollen,[1,2] S. E. Campbell,[1,2] X. Chen,[1] H. Erington,[1,2] N. D. Gamage,[1] M. J. Gutiérrez,[3,4] C. Izzo,[1] E. Leistenschneider,[5] E. M. Lykiardopoulou,[5] R. Orford,[5] W. S. Porter,[6] D. Puentes,[1,2] M. Redshaw,[7] R. Ringle,[1,2] S. Rogers,[1] S. Schwarz,[1] L. Stackable,[1] C. S. Sumithrarachchi,[1] A. A. Valverde,[8] A. C. C. Villari,[1] and I. T. Yandow[1,2]

[1]*Facility for Rare Isotope Beams, East Lansing, Michigan 48824, USA*
[2]*Department of Physics and Astronomy, Michigan State University, East Lansing, Michigan 48824, USA*
[3]*Institut für Physik, Universität Greifswald, 17487 Greifswald, Germany*
[4]*GSI Helmholtzzentrum für Schwerionenforschung, D-64291 Darmstadt, Germany*
[5]*Nuclear Science Division, Lawrence Berkeley National Laboratory, Berkeley, California 94720, USA*
[6]*Department of Physics and Astronomy, University of Notre Dame, Notre Dame, Indiana 46556, USA*
[7]*Department of Physics, Central Michigan University, Mount Pleasant, Michigan 48859, USA*
[8]*Physics Divison, Argonne National Laboratory, Lemont, Illinois 60439, USA*

(Received 6 October 2024; accepted 12 November 2024; published 9 January 2025)

As a step towards the ultimate goal of a high-precision mass measurement of doubly magic ^{100}Sn, the mass of ^{103}Sn was measured at the Low Energy Beam and Ion Trap (LEBIT) located at the Facility for Rare Isotope Beams (FRIB). Utilizing the time-of-flight ion cyclotron resonance technique, a mass uncertainty of 3.7 keV was achieved, an improvement by more than an order of magnitude compared to a recent measurement performed in 2023 at the Cooler Storage Ring (CSRe) in Lanzhou. Although the LEBIT and CSRe mass measurements of ^{103}Sn are in agreement, they diverge from the experimental mass value reported in the 2016 version of the Atomic Mass Evaluation (AME2016), which was derived from the measured Q_{β^+} value and the mass of ^{103}In. In AME2020, this indirectly measured ^{103}Sn mass was classified as a "seriously irregular mass" and replaced with an extrapolated value, which aligns with the most recent measured values from CSRe and LEBIT. As such, the smoothness of the mass surface is confidently reestablished for ^{103}Sn. Furthermore, LEBIT's mass measurement of ^{103}Sn enabled a significant reduction in the mass uncertainties of five parent isotopes which are now dominated by uncertainties in their respective Q values.

DOI: 10.1103/PhysRevC.111.014314

I. INTRODUCTION

Atomic nuclei composed of specific numbers of protons and neutrons known as magic numbers show particularly energetically favorable configurations. For example, the binding energy of these nuclei is significantly higher than what the semiempirical mass formula [1], derived from the liquid drop model of the nucleus, would predict. Understanding the microscopic origins of this phenomenon, known as nuclear shell evolution, is a central focus of contemporary nuclear physics [2,3]. The isotope ^{100}Sn is often referred to as the "holy grail of nuclear structure research," as it is the heaviest known proton-bound nucleus among the self-conjugate ($N = Z$) nuclei, which is expected to be doubly magic with neutron and proton shell closures at $N = 50$ and $Z = 50$, respectively. Comprehensive reviews of the existing literature on ^{100}Sn can be found in Refs. [4,5]. Significant experimental efforts are under way to measure the properties of ^{100}Sn. Its proximity to the proton drip-line makes it one of the rarest nuclei to study. As such, only its half-life, β-endpoint energy, and mass are known so far [6,7]. Unfortunately, the limited precision of the latter does not provide sufficient clarity regarding the nuclear shell evolution along the proton drip-line.

The properties of nuclei close to ^{100}Sn are also of high interest for nuclear structure studies (see, e.g., recent discussions in Refs. [8–13]). The isotopes located northeast of ^{100}Sn on the nuclear chart form an island of enhanced α and proton decay whose existence originates from the double magicity of ^{100}Sn and the proximity to the proton drip-line [14]. They show a large Gamow-Teller β-decay strength [6], superallowed α decay [15–20], and potentially cluster [21–23] and two-proton emission [24,25]. Moreover, these isotopes play a role in stellar nucleosynthesis as the astrophysical rapid proton (rp) capture process dies out in this region [14,26–30]. Precise knowledge of their binding energies, and thus their masses, is necessary to establish the energy balances of the relevant decays and transitions in this process.

Since the decay chains of ^{104}Sb, ^{107}Te, ^{108}I, ^{111}Xe, and ^{112}Cs are terminated in ^{103}Sn (see Fig. 1), a precise knowledge of the mass of ^{103}Sn is required to determine the masses of these five isotopes based on their respective Q values known from decay spectroscopy [31]. However, the mass of ^{103}Sn has been a topic of debate. The 2016 version of the Atomic

*Contact author: ireland@frib.msu.edu

 ©2025 American Physical Society

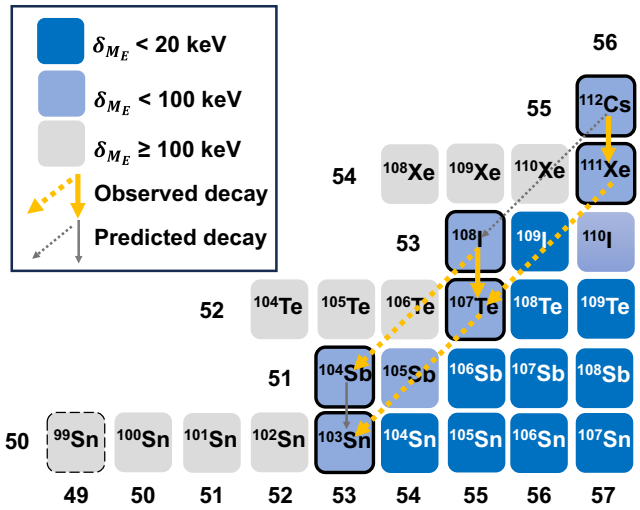

FIG. 1. The nuclear landscape in the region of ^{100}Sn. Individual isotopes are colored based on their mass excess uncertainties δ_{M_E} prior to this work. A dashed border around an isotope refers to an extrapolated mass. The mass excesses of isotopes marked with a thick solid border were improved in this work. Directly observed and predicted decay chains are illustrated by thick orange and thin gray arrows, respectively, representing either proton (solid arrows) or α (dashed arrows) decay.

Mass Evaluation (AME2016) [32] reported an experimental mass excess of −66 970(70) keV for ^{103}Sn derived from the Q_{β^+} value and the mass of ^{103}In, but significant inconsistencies with theoretical predictions (see, e.g., Ref. [8]), and mass surface trends led to its replacement with an extrapolated value of −67 090(100) keV in AME2020 [31]. A subsequent direct mass measurement at the Cooler Storage Ring (CSRe) in Lanzhou in 2023 yielded a mass excess of −67 138(68) keV [33], which is in good agreement with the extrapolated value in AME2020, restoring confidence in the smoothness of the mass surface. An independent and more precise mass measurement of ^{103}Sn would further validate this finding and would serve as a crucial anchor for the masses of ^{104}Sb, ^{107}Te, ^{108}I, ^{111}Xe, and ^{112}Cs.

In this work, we report on high-precision Penning-trap mass measurements of ^{103}Sn performed at the Low Energy Beam and Ion Trap (LEBIT) [34] located at the Facility of Rare Isotope Beams (FRIB) using the time-of-flight ion cyclotron resonance (ToF-ICR) technique [35–37]. Beyond its relevance to nuclear structure and astrophysics, the high-precision mass measurement of ^{103}Sn serves as a step towards a measurement of ^{100}Sn. With the ongoing ramp-up of beam intensity [38], FRIB is expected to produce ^{100}Sn, as well as many of its neighbors, at rates of a few ions per second in the near future, paving the way for exceptional research opportunities and deeper insights into the evolution of the nuclear shells in the vicinity of doubly magic ^{100}Sn.

II. EXPERIMENTAL METHOD AND ANALYSIS

A beam of radioactive ^{103}Sn was produced via projectile fragmentation. A ^{124}Xe primary beam was accelerated in FRIB's superconducting linear accelerator [39] to an energy of 228 MeV/u and sent to a 2.015-mm-thick ^{12}C target, creating a cocktail of ion species that was passed to the Advanced Rare Isotope Separator (ARIS) [40] for purification. In preparation for stopping the ions in a gas stopper, the momentum of the purified beam was compressed using an Al wedge of 1004 μm in thickness at an angle of 2.67 mrad, followed by a 611-μm-thick Al degrader. An optimal degrader angle of 17° was determined by adjusting the effective thickness seen by the incoming beam. This process prepared the beam for acceptance into the Advanced Cryogenic Gas Stopper (ACGS) [41], which utilizes helium buffer gas to stop the beam. After stopping, radio-frequency (rf) carpet surfing [42] was used to guide the ions to an extraction orifice. After extraction, the ions passed through a buffer-gas filled rf quadrupole with differential pumping and were accelerated to 30 keV. The energy spread of the ion beam after the rf quadrupole was a few electron volts. The ratio of singly charged to doubly charged ^{103}Sn ions out of the ACGS was approximately 1:1. A dipole magnet with resolving power ≈1500 selected all ion species with a mass-to-charge ratio of $A/Q = 51.5$. The choice of a half-integer A/Q was motivated to deliver pure ^{103}Sn^{2+} to LEBIT. At LEBIT, the continuous ion beam was injected into a linear buffer-gas-filled Paul-trap cooler-buncher [43] for accumulation, cooling and bunching of the ion beam. Following the extraction of the ions from the Paul trap as well-defined ion bunches with reduced emittance, the ions were guided into LEBIT's 9.4-T hyperbolic Penning trap [44]. The ion rate detected at a microchannel-plate (MCP) detector located downstream of the Penning trap was on average 0.25 ions/s.

In the Penning trap, the ions were confined in three dimensions by a homogeneous magnetic field B and a quadrupolar electrostatic field. The motion of an ion in a Penning trap is characterized by three eigenfrequencies: an axial frequency ν_z and two radial frequencies, ν_- (magnetron frequency) and ν_+ (reduced-cyclotron frequency), where typically $\nu_- \ll \nu_z < \nu_+$. For an ideal trap, the cyclotron frequency ν_c of an ion can be approximated as the sum of its radial frequencies [45],

$$\nu_c = \nu_+ + \nu_-. \tag{1}$$

Penning traps enable a precise determination of the mass m of the ion of interest by measuring its cyclotron frequency $\nu_c = qB/(2\pi m)$ relative to that of a well-known reference ion: $\nu_{c,\mathrm{ref}} = q_{\mathrm{ref}}B/(2\pi m_{\mathrm{ref}})$. The cyclotron frequency ratio R is given by

$$R = \frac{\nu_c}{\nu_{c,\mathrm{ref}}} = \frac{q m_{\mathrm{ref}}}{q_{\mathrm{ref}} m}, \tag{2}$$

where q and q_{ref} are the charges and m and m_{ref} are the masses of the ion of interest and the reference ion, respectively.

In this work, the mass of ^{103}Sn^{2+} was determined using the ToF-ICR technique [35–37]. Extracted ions from the cooler-buncher were steered off-axis relative to the trap center upon injection into the Penning trap using a Lorentz steerer [46], inducing the initial magnetron motion. A quadrupolar rf pulse applied for an excitation time of 250 ms within a frequency range near that of the expected cyclotron frequency

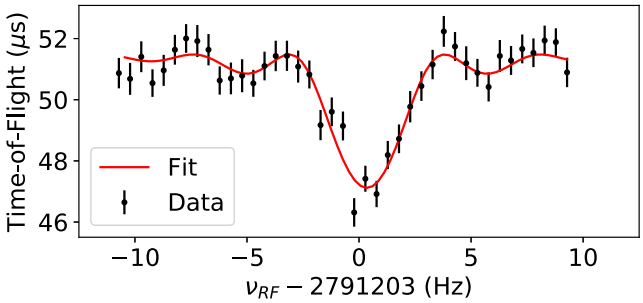

FIG. 2. A summed ToF-ICR spectrum of all eight individual cyclotron frequency measurements taken for $^{103}Sn^{2+}$ using the LEBIT 9.4-T Penning trap mass spectrometer. A χ^2 minimization fit to the analytical curve described in Ref. [37], depicted in red, was used to determine the frequency $\nu_{rf} = \nu_c$ occurring at the minimum time-of-flight. The width of the central dip corresponds to the inverse of the applied 250-ms quadrupolar excitation time.

for $^{103}Sn^{2+}$ converted the slow magnetron motion to fast reduced cyclotron motion. The ions were subsequently ejected and their time-of-flight to the MCP detector was recorded. Figure 2 shows the ions' time-of-flight as a function of the applied quadrupolar frequency ν_{rf}. When ν_{rf} approached ν_c, the ions' radial energy increased, resulting in a shorter flight time to the detector. This led to a time-of-flight minimum when $\nu_{rf} = \nu_c$. Measurements of the ion of interest for 250 ms of quadrupolar excitation time and measurements of the stable molecular reference $^{12}C_3\,^{1}H_2\,^{14}N_1^+$ for 500 ms of excitation time were interleaved to yield the average ratio $\bar{R}$, weighted by each measurement's uncertainty. The mass of ^{103}Sn was determined according to Eq. (2), accounting for the mass of the missing electron(s). The electron's binding energy itself was neglected, as it was smaller than the statistical uncertainty of $\bar{R}$.

III. RESULTS

Eight ToF-ICR measurements of $^{103}Sn^{2+}$ were taken over the course of approximately 8 h. Each individual measurement of $^{103}Sn^{2+}$ lasted for around 30 min, interleaved with 8-min-long measurements of the stable molecular reference. The measured frequency ratios of the individual measurements

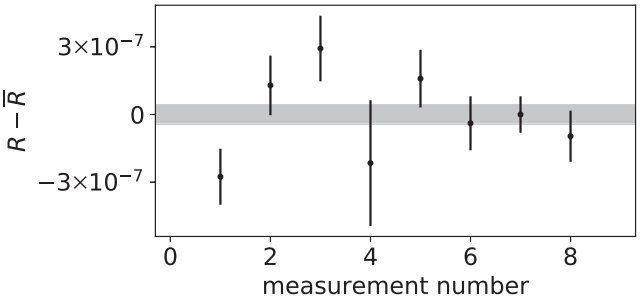

FIG. 3. Cyclotron frequency ratios R with respect to the average ratio $\bar{R} = 1.010\,779\,605(29)$. The gray bar shows the $\pm1\sigma$ uncertainty in $\bar{R}$.

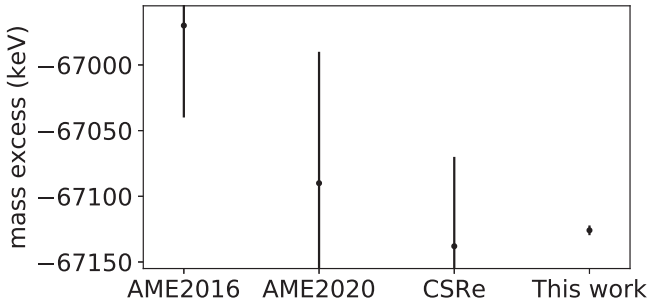

FIG. 4. Mass excess for ^{103}Sn compared with the literature (AME2016 [32], AME2020 [31], and CSRe [33]).

are shown in Fig. 3 relative to those of the stable reference. The weighted average mass ratio $\bar{R} = 1.010\,779\,605(29)$ corresponds to a mass excess of $-67\,125.9(3.7)$ keV for ^{103}Sn.

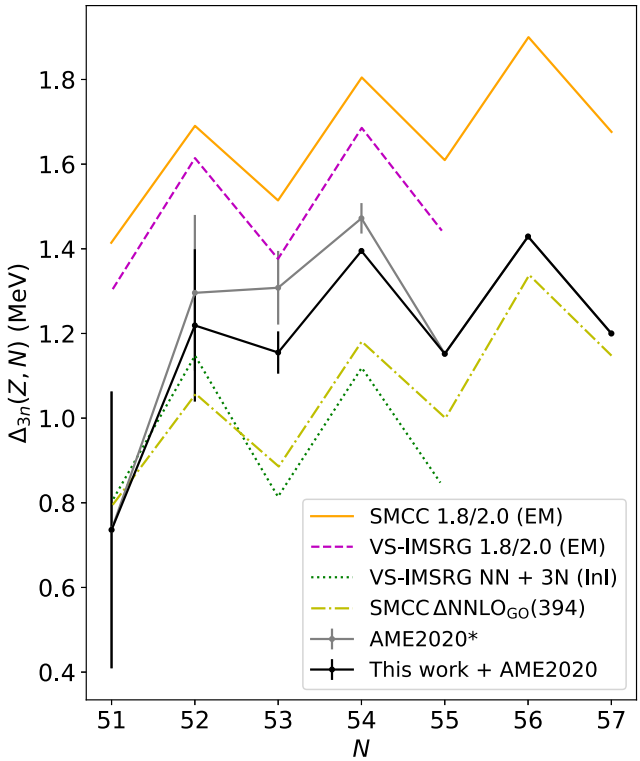

FIG. 5. Three-point estimator for the odd-even staggering for the tin isotopic chain ($Z = 50$) as a function of neutron number N. The experimental data (gray and black curves) are taken from AME2020 [31] except for ^{103}Sn. The black curve takes our new mass measurement of ^{103}Sn into account. The gray curve utilizes the experimental mass of ^{103}Sn as reported in AME2016 [32], which was replaced with an extrapolated value in AME2020. Besides the mass of ^{103}Sn, the masses reported in AME2020 are used. The theoretical results of the valence-space formulation of the in-medium similarity renormalization group (VS-IMSRG) as well as of the shell-model coupled-cluster (SMCC) calculations are taken from Ref. [8]. The uncertainties on the theoretical calculations are estimated to be 0.1 MeV for the VS-IMSRG calculations and 0.2 MeV for the SMCC calculations [8].

TABLE I. Measured Q values as reported in AME2020 [31] and used for the mass excess calculation of the five parent isotopes of ^{103}Sn presented in Table II.

	Q value (keV)	References
$Q_p(^{108}\mathrm{I})$	597(13)	[26]
$Q_p(^{112}\mathrm{Cs})$	816(4)	[51,52]
$Q_\alpha(^{107}\mathrm{Te})$	4010(5)	[26,53–55]
$Q_\alpha(^{108}\mathrm{I})$	4099(5)	[26,51]
$Q_\alpha(^{111}\mathrm{Xe})$	3710(60)	[53–56]

TABLE II. Measured mass excess of ^{103}Sn and calculated mass excesses based on the ^{103}Sn measurement from this work (left column) compared to the result from CSRe [33] (right column).

	$M_{E,\mathrm{LEBIT}}$ (keV)	$M_{E,\mathrm{CSRe}}$ (keV)
^{103}Sn	−67 125.9(3.7)	−67 138(68)
^{104}Sb	−59 329(15)	−59 340(70)
^{107}Te	−60 691(6)	−60 700(70)
^{108}I	−52 805(14)	−52 820(70)
^{111}Xe	−54 556(60)	−54 570(90)
^{112}Cs	−46 451(60)	−46 460(90)

Several systematic effects add an uncertainty δ_R to $\bar{R}$. Mass-dependent shifts related to inhomogeneity in the magnetic field and trap imperfections were studied at LEBIT in detail and are known to add an uncertainty of $\delta_R \approx 2 \times 10^{-10}/u$ [47]. Additionally, nonlinear temporal shifts in the magnetic field at LEBIT contribute $\delta_R < 10^{-9}$ per hour [48]. To counter these, regular reference measurements were performed. The maximum ion cutoff $\leqslant 5$ also allowed the uncertainty due to ion-ion interactions to be $\delta_R \approx 10^{-8}$. These various uncertainties are negligible in comparison to the statistical precision of the measurement ($\approx 10^{-7}$). The cyclotron frequency ratio R was periodically checked against the expected R determined from masses obtained from AME2020 as measurements were performed to verify that it did not correspond to (molecular) isobars within the uncertainty of the measurement. No such isobars were plausible, providing confirmation that what was measured was indeed $^{103}\mathrm{Sn}^{2+}$.

IV. DISCUSSION

Our mass value of ^{103}Sn agrees with the previous measurement conducted at CSRe [33], while improving the precision by more than an order of magnitude (see Fig. 4). However, both of these measurements deviate from the mass reported experimentally in AME2016 [32], which was derived indirectly from the known mass of ^{103}In and the β-decay energy Q_{β^+} between ^{103}Sn and ^{103}In [32,49,50]. Assuming that the atomic mass M of ^{103}In is well known, we calculate a new Q_{β^+} value based on our measured mass of ^{103}Sn and the AME2020 mass of ^{103}In [31], $Q_{\beta^+} = M(^{103}\mathrm{Sn}) - M(^{103}\mathrm{In})$. Our updated Q_{β^+} value is 7506(10) keV, compared to the previous value of 7660(70) keV. This discrepancy indicates a limited understanding of the full decay processes, possibly due to internal γ conversion or undetected weak-decay branches in Refs. [49,50]. In AME2020 [31], the mass of ^{103}Sn was classified as a "seriously irregular mass" and replaced by an extrapolated value, which perfectly matches our new measurement. Consequently, the smoothness of the mass surface around ^{103}Sn is confidently restored. Taking our new mass value of ^{103}Sn into account, the experimental trend of the three-point estimator for the odd-even staggering $\Delta_{3n}(Z,N) = 0.5(-1)^N[M_E(Z,N-1) - 2M_E(Z,N) + M_E(Z,N+1)]$ along the tin isotopic chain is relatively well reproduced by various theoretical models that are discussed in detail in Ref. [8] (see Fig. 5). This increases confidence in the predictive power of these theoretical calculations for ^{100}Sn.

Furthermore, our new high-precision mass measurement of ^{103}Sn significantly reduces the mass uncertainty of the α and proton emitters ^{104}Sb, ^{107}Te, ^{108}I, ^{111}Xe, and ^{112}Cs, which are located northeast of the nuclear chart with respect to ^{100}Sn (see Fig. 1). The mass excesses of these five isotopes were calculated based on our high-precision ^{103}Sn measurement and the respective Q values (see Table I):

$$\begin{aligned} M_E(^{107}\mathrm{Te}) &= M_E(^{103}\mathrm{Sn}) + M_E(\alpha) + Q_\alpha(^{107}\mathrm{Te}),\\ M_E(^{111}\mathrm{Xe}) &= M_E(^{107}\mathrm{Te}) + M_E(\alpha) + Q_\alpha(^{111}\mathrm{Xe}),\\ M_E(^{112}\mathrm{Cs}) &= M_E(^{111}\mathrm{Xe}) + M_E(p) + Q_p(^{112}\mathrm{Cs}),\\ M_E(^{108}\mathrm{I}) &= M_E(^{107}\mathrm{Te}) + M_E(p) + Q_p(^{108}\mathrm{I}),\ \text{and}\\ M_E(^{104}\mathrm{Sb}) &= M_E(^{108}\mathrm{I}) - M_E(\alpha) - Q_\alpha(^{108}\mathrm{I}). \end{aligned} \tag{3}$$

Tables II and III show the respective mass excesses, compared against the values from CSRe [33] and the extrapolated values in AME2020 [31], respectively. Their uncertainties are now dominated by the uncertainties of the respective Q values and not by the uncertainty in the mass excess of ^{103}Sn. Precise mass determinations, and ideally direct mass measurements in the future, aid in establishing the energy balances of the relevant decays and transitions.

V. CONCLUSIONS

The first Penning-trap mass measurement of ^{103}Sn was performed at LEBIT [34] and a mass excess of

TABLE III. Measured mass excess of ^{103}Sn and calculated mass excesses based on the ^{103}Sn measurement from this work (left column) compared to the result from AME2020 [57] (right column).

	$M_{E,\mathrm{LEBIT}}$ (keV)	$M_{E,\mathrm{AME2020}}$ (keV)
^{103}Sn	−67 125.9(3.7)	−67 090(100)[a]
^{104}Sb	−59 329(15)	−59 300(100)[a]
^{107}Te	−60 691(6)	−60 660(100)[a]
^{108}I	−52 805(14)	−52 770(100)[a]
^{111}Xe	−54 556(60)	−54 520(120)[a]
^{112}Cs	−46 451(60)	−46 420(120)[a]

[a]Indicates an estimated value based on the trends from the mass surface.

−67 125.9(3.7) keV was obtained. This value improves the precision of the previous measurement [33] by more than an order of magnitude and restores confidence in the smoothness of the nuclear mass surface. Furthermore, the masses of five parent α or proton emitters calculated from this improved measurement of ^{103}Sn have become well-anchored and their mass uncertainties are now dominated by their respective Q values. The closed neutron and proton shells at $N = 50$ and $Z = 50$ of ^{100}Sn provide a unique testing ground for our understanding of nuclear forces and shell evolution. Our measurement of ^{103}Sn, just three neutrons away from ^{100}Sn, lays the foundation for future high-precision mass measurements of ^{100}Sn.

ACKNOWLEDGMENTS

This material is based upon work supported by the U.S. Department of Energy, Office of Science, Office of Nuclear Physics, and used resources of the Facility for Rare Isotope Beams (FRIB) Operations, which is a DOE, Office of Science, User Facility under Award No. DE-SC0023633. This work was conducted with the support of Michigan State University; the U.S. National Science Foundation under Contracts No. PHY-1565546 and No. PHY-2111185; and the DOE, Office of Nuclear Physics, under Contracts No. DE-AC02-06CH11357, No. DE-AC02-05CH11231, and No. DE-SC0022538. S.E.C. acknowledges support from the DOE NNSA SSGF under Contract No. DE-NA0003960.

[1] D. Benzaid, S. Bentridi, A. Kerraci, and N. Amrani, Bethe–Weizsäcker semiempirical mass formula coefficients 2019 update based on AME2016, Nucl. Sci. Tech. **31**, 9 (2020).

[2] O. Sorlin and M.-G. Porquet, Nuclear magic numbers: New features far from stability, Prog. Part. Nucl. Phys. **61**, 602 (2008).

[3] R. Kanungo, A new view of nuclear shells, Phys. Scr. **2013**, 014002 (2013).

[4] T. Faestermann, M. Górska, and H. Grawe, The structure of ^{100}Sn and neighbouring nuclei, Prog. Part. Nucl. Phys. **69**, 85 (2013).

[5] M. Górska, Trends in the structure of nuclei near ^{100}Sn, Physics **4**, 364 (2022).

[6] C. Hinke, M. Böhmer, P. Boutachkov, T. Faestermann, H. Geissel, J. Gerl, R. Gernhäuser, M. Górska, A. Gottardo, H. Grawe *et al.*, Superallowed Gamow–Teller decay of the doubly magic nucleus ^{100}Sn, Nature (London) **486**, 341 (2012).

[7] M. Chartier, G. Auger, W. Mittig, A. Lépine-Szily, L. K. Fifield, J. M. Casandjian, M. Chabert, J. Fermé, A. Gillibert, M. Lewitowicz, M. Mac Cormick, M. H. Moscatello, O. H. Odland, N. A. Orr, G. Politi, C. Spitaels, and A. C. C. Villari, Mass measurement of ^{100}Sn, Phys. Rev. Lett. **77**, 2400 (1996).

[8] M. Mougeot, D. Atanasov, J. Karthein, R. N. Wolf, P. Ascher, K. Blaum, K. Chrysalidis, G. Hagen, J. D. Holt, W. J. Huang, G. R. Jansen, I. Kulikov, Y. A. Litvinov, D. Lunney, V. Manea, T. Miyagi, T. Papenbrock, L. Schweikhard, A. Schwenk, T. Steinsberger *et al.*, Mass measurements of $^{99-101}$In challenge *ab initio* nuclear theory of the nuclide ^{100}Sn, Nat. Phys. **17**, 1099 (2021).

[9] L. Nies, D. Atanasov, M. Athanasakis-Kaklamanakis, M. Au, K. Blaum, J. Dobaczewski, B. S. Hu, J. D. Holt, J. Karthein, I. Kulikov, Y. A. Litvinov, D. Lunney, V. Manea, T. Miyagi, M. Mougeot, L. Schweikhard, A. Schwenk, K. Sieja, and F. Wienholtz, Isomeric excitation energy for ^{99}In^{m} from mass spectrometry reveals constant trend next to doubly magic ^{100}Sn, Phys. Rev. Lett. **131**, 022502 (2023).

[10] J. Park, R. Krücken, A. Blazhev, D. Lubos, R. Gernhäuser, M. Lewitowicz, S. Nishimura, D. S. Ahn, H. Baba, B. Blank, P. Boutachkov, F. Browne, I. Čeliković, G. de France, P. Doornenbal, T. Faestermann, Y. Fang, N. Fukuda, J. Giovinazzo, N. Goel *et al.*, Spectroscopy of ^{99}Cd and ^{101}In from β decays of ^{99}In and ^{101}Sn, Phys. Rev. C **102**, 014304 (2020).

[11] M. Reponen, R. P. de Groote, L. Al Ayoubi, O. Beliuskina, M. L. Bissell, P. Campbell, L. Cañete, B. Cheal, K. Chrysalidis, C. Delafosse, A. de Roubin, C. S. Devlin, T. Eronen, R. F. Garcia Ruiz, S. Geldhof, W. Gins, M. Hukkanen, P. Imgram, A. Kankainen, M. Kortelainen *et al.*, Evidence of a sudden increase in the nuclear size of proton-rich silver-96, Nat. Commun. **12**, 4596 (2021).

[12] C. Hornung, D. Amanbayev, I. Dedes, G. Kripko-Koncz, I. Miskun, N. Shimizu, S. Ayet San Andrés, J. Bergmann, T. Dickel, J. Dudek, J. Ebert, H. Geissel, M. Górska, H. Grawe, F. Greiner, E. Haettner, T. Otsuka, W. R. Plaß, S. Purushothaman, A.-K. Rink *et al.*, Isomer studies in the vicinity of the doubly-magic nucleus ^{100}Sn: Observation of a new low-lying isomeric state in ^{97}Ag, Phys. Lett. B **802**, 135200 (2020).

[13] J. Karthein, C. M. Ricketts, R. F. Garcia Ruiz, J. Billowes, C. L. Binnersley, T. E. Cocolios, J. Dobaczewski, G. J. Farooq-Smith, K. T. Flanagan, G. Georgiev *et al.*, Electromagnetic properties of indium isotopes illuminate the doubly magic character of ^{100}Sn, Nat. Phys. **20**, 1719 (2024).

[14] L. Cartegni, C. Mazzocchi, R. Grzywacz, I. G. Darby, S. N. Liddick, K. P. Rykaczewski, J. C. Batchelder, L. Bianco, C. R. Bingham, E. Freeman, C. Goodin, C. J. Gross, A. Guglielmetti, D. T. Joss, S. H. Liu, M. Mazzocco, S. Padgett, R. D. Page, M. M. Rajabali, M. Romoli *et al.*, Experimental study of the decays of ^{112}Cs and ^{111}Xe, Phys. Rev. C **85**, 014312 (2012).

[15] K. Auranen, D. Seweryniak, M. Albers, A. D. Ayangeakaa, S. Bottoni, M. P. Carpenter, C. J. Chiara, P. Copp, H. M. David, D. T. Doherty, J. Harker, C. R. Hoffman, R. V. F. Janssens, T. L. Khoo, S. A. Kuvin, T. Lauritsen, G. Lotay, A. M. Rogers, J. Sethi, C. Scholey *et al.*, Superallowed α decay to doubly magic ^{100}Sn, Phys. Rev. Lett. **121**, 182501 (2018).

[16] R. D. Macfarlane and A. Siivola, New region of alpha radioactivity, Phys. Rev. Lett. **14**, 114 (1965).

[17] D. Seweryniak, K. Starosta, C. N. Davids, S. Gros, A. A. Hecht, N. Hoteling, T. L. Khoo, K. Lagergren, G. Lotay, D. Peterson, A. Robinson, C. Vaman, W. B. Walters, P. J. Woods, and S. Zhu, α decay of ^{105}Te, Phys. Rev. C **73**, 061301(R) (2006).

[18] S. N. Liddick, R. Grzywacz, C. Mazzocchi, R. D. Page, K. P. Rykaczewski, J. C. Batchelder, C. R. Bingham, I. G. Darby, G. Drafta, C. Goodin, C. J. Gross, J. H. Hamilton, A. A. Hecht, J. K. Hwang, S. Ilyushkin, D. T. Joss, A. Korgul, W. Królas, K. Lagergren, K. Li *et al.*, Discovery of ^{109}Xe and ^{105}Te: Superallowed α decay near doubly magic ^{100}Sn, Phys. Rev. Lett. **97**, 082501 (2006).

[19] Z. Janas, C. Mazzocchi, L. Batist, A. Blazhev, M. Górska, M. Kavatsyuk, O. Kavatsyuk, R. Kirchner, A. Korgul, M. La Commara, K. Miernik, I. Mukha, A. Płochocki, E. Roeckl, and K. Schmidt, Measurements of ^{110}Xe and ^{106}Te decay half-lives, Eur. Phys. J. A **23**, 197 (2005).

[20] L. Capponi, J. F. Smith, P. Ruotsalainen, C. Scholey, P. Rahkila, K. Auranen, L. Bianco, A. J. Boston, H. C. Boston, D. M. Cullen, X. Derkx, M. C. Drummond, T. Grahn, P. T. Greenlees, L. Grocutt, B. Hadinia, U. Jakobsson, D. T. Joss, R. Julin, S. Juutinen *et al.*, Direct observation of the ^{114}Ba → ^{110}Xe → ^{106}Te → ^{102}Sn triple α-decay chain using position and time correlations, Phys. Rev. C **94**, 024314 (2016).

[21] A. Florescu and A. Insolia, Microscopic calculation for α and heavier cluster emissions from proton rich Ba and Ce isotopes, Phys. Rev. C **52**, 726 (1995).

[22] S. Kumar and R. K. Gupta, Measurable decay modes of barium isotopes via exotic cluster emissions, Phys. Rev. C **49**, 1922 (1994).

[23] S. Kumar, D. Bir, and R. K. Gupta, ^{100}daughter α-nuclei cluster decays of some neutron-deficient Xe to Gd parents: Sn radioactivity, Phys. Rev. C **51**, 1762 (1995).

[24] J. Dobaczewski and W. Nazarewicz, Limits of proton stability near ^{100}Sn, Phys. Rev. C **51**, R1070 (1995).

[25] E. Olsen, M. Pfützner, N. Birge, M. Brown, W. Nazarewicz, and A. Perhac, Landscape of two-proton radioactivity, Phys. Rev. Lett. **110**, 222501 (2013).

[26] K. Auranen, D. Seweryniak, M. Albers, A. Ayangeakaa, S. Bottoni, M. Carpenter, C. Chiara, P. Copp, H. David, D. Doherty, J. Harker, C. Hoffman, R. Janssens, T. Khoo, S. Kuvin, T. Lauritsen, G. Lotay, A. Rogers, C. Scholey, J. Sethi *et al.*, Proton decay of ^{108}I and its significance for the termination of the astrophysical *rp*-process, Phys. Lett. B **792**, 187 (2019).

[27] H. Schatz, A. Aprahamian, V. Barnard, L. Bildsten, A. Cumming, M. Ouellette, T. Rauscher, F.-K. Thielemann, and M. Wiescher, End point of the *rp* process on accreting neutron stars, Phys. Rev. Lett. **86**, 3471 (2001).

[28] V.-V. Elomaa, G. K. Vorobjev, A. Kankainen, L. Batist, S. Eliseev, T. Eronen, J. Hakala, A. Jokinen, I. D. Moore, Y. N. Novikov, H. Penttilä, A. Popov, S. Rahaman, J. Rissanen, A. Saastamoinen, H. Schatz, D. M. Seliverstov, C. Weber, and J. Äystö, Quenching of the SnSbTe cycle in the *rp* process, Phys. Rev. Lett. **102**, 252501 (2009).

[29] H. Grawe, K. Langanke, and G. Martínez-Pinedo, Nuclear structure and astrophysics, Rep. Prog. Phys. **70**, 1525 (2007).

[30] C. Mazzocchi, R. Grzywacz, S. N. Liddick, K. P. Rykaczewski, H. Schatz, J. C. Batchelder, C. R. Bingham, C. J. Gross, J. H. Hamilton, J. K. Hwang, S. Ilyushkin, A. Korgul, W. Królas, K. Li, R. D. Page, D. Simpson, and J. A. Winger, α Decay of ^{109}I and its implications for the proton decay of ^{105}Sb and the astrophysical rapid proton-capture process, Phys. Rev. Lett. **98**, 212501 (2007).

[31] M. Wang, W. Huang, F. Kondev, G. Audi, and S. Naimi, The AME 2020 atomic mass evaluation (II). Tables, graphs and references, Chin. Phys. C **45**, 030003 (2021).

[32] W. Meng, G. Audi, F. G. Kondev, W. Huang, S. Naimi, and X. Xing, The AME2016 atomic mass evaluation (II). Tables, graphs and references, Chin. Phys. C **41**, 030003 (2017).

[33] Y. M. Xing, C. X. Yuan, M. Wang, Y. H. Zhang, X. H. Zhou, Y. A. Litvinov, K. Blaum, H. S. Xu, T. Bao, R. J. Chen, C. Y. Fu, B. S. Gao, W. W. Ge, J. J. He, W. J. Huang, T. Liao, J. G. Li, H. F. Li, S. Litvinov, S. Naimi *et al.*, Isochronous mass measurements of neutron-deficient nuclei from ^{112}Sn projectile fragmentation, Phys. Rev. C **107**, 014304 (2023).

[34] R. Ringle, S. Schwarz, and G. Bollen, Penning trap mass spectrometry of rare isotopes produced via projectile fragmentation at the LEBIT facility, Int. J. Mass Spectrom. **349–350**, 87 (2013).

[35] G. Bollen, R. B. Moore, G. Savard, and H. Stolzenberg, The accuracy of heavy-ion mass measurements using time of flight-ion cyclotron resonance in a Penning trap, J. Appl. Phys. **68**, 4355 (1990).

[36] S. Becker *et al.* (Isolde Collaboration), Mass measurements of very high accuracy by time-of-flight ion cyclotron resonance of ions injected into a Penning trap, Int. J. Mass Spectrom. Ion Process. **99**, 53 (1990).

[37] M. König, G. Bollen, H.-J. Kluge, T. Otto, and J. Szerypo, Quadrupole excitation of stored ion motion at the true cyclotron frequency, Int. J. Mass Spectrom. Ion Process. **142**, 95 (1995).

[38] J. Wei, H. Ao, B. Arend, S. Beher, G. Bollen, N. Bultman, F. Casagrande, W. Chang, Y. Choi, S. Cogan, C. Compton, M. Cortesi, J. Curtin, K. Davidson, X. Du, K. Elliott, B. Ewert, A. Facco, A. Fila, K. Fukushima *et al.*, Accelerator commissioning and rare isotope identification at the facility for rare isotope beams, Mod. Phys. Lett. A **37**, 2230006 (2022).

[39] R. York, G. Bollen, C. Compton, A. Crawford, M. Doleans, T. Glasmacher, W. Hartung, F. Marti, J. Popielarski, J. Vincent *et al.*, FRIB: A new accelerator facility for the production of rare isotope beams, SRF2009, Berlin, September, 2009.

[40] M. Hausmann, A. M. Aaron, A. M. Amthor, M. Avilov, L. Bandura, R. Bennett, G. Bollen, T. Borden, T. W. Burgess, S. S. Chouhan *et al.*, Design of the Advanced Rare Isotope Separator ARIS at FRIB, Nucl. Instrum. Methods Phys. Res. Sect. B **317**, 349 (2013).

[41] K. R. Lund, G. Bollen, D. Lawton, D. J. Morrissey, J. Ottarson, R. Ringle, S. Schwarz, C. S. Sumithrarachchi, A. C. C. Villari, and J. Yurkon, Online tests of the advanced cryogenic gas stopper at NSCL, Nucl. Instrum. Methods Phys. Res. Sect. B **463**, 378 (2020).

[42] G. Bollen, "Ion surfing" with radiofrequency carpets, Int. J. Mass Spectrom. **299**, 131 (2011).

[43] S. Schwarz, G. Bollen, R. Ringle, J. Savory, and P. Schury, The LEBIT ion cooler and buncher, Nucl. Instrum. Methods Phys. Res. Sect. A **816**, 131 (2016).

[44] R. Ringle, G. Bollen, A. Prinke, J. Savory, P. Schury, S. Schwarz, and T. Sun, The LEBIT 9.4T Penning trap mass spectrometer, Nucl. Instrum. Methods Phys. Res. Sect. A **604**, 536 (2009).

[45] G. Gabrielse, Why is sideband mass spectrometry possible with ions in a Penning trap? Phys. Rev. Lett. **102**, 172501 (2009).

[46] R. Ringle, G. Bollen, A. Prinke, J. Savory, P. Schury, S. Schwarz, and T. Sun, A "Lorentz" steerer for ion injection into a Penning trap, Int. J. Mass Spectrom. **263**, 38 (2007).

[47] K. Gulyuz, J. Ariche, G. Bollen, S. Bustabad, M. Eibach, C. Izzo, S. J. Novario, M. Redshaw, R. Ringle, R. Sandler, S. Schwarz, and A. A. Valverde, Determination of the direct double-β-decay Q value of ^{96}Zr and atomic masses of $^{90-92,94,96}$Zr and $^{92,94-98,100}$Mo, Phys. Rev. C **91**, 055501 (2015).

[48] R. Ringle, T. Sun, G. Bollen, D. Davies, M. Facina, J. Huikari, E. Kwan, D. J. Morrissey, A. Prinke, J. Savory, P. Schury, S. Schwarz, and C. S. Sumithrarachchi, High-precision Penning trap mass measurements of ^{37,38}Ca and their contributions to

conserved vector current and isobaric mass multiplet equation, Phys. Rev. C **75**, 055503 (2007).

[49] I. Mukha, L. Batist, F. Becker, A. Blazhev, A. Brüchle, J. Döring, M. Górska, H. Grawe, T. Faestermann, C. Hoffman *et al.*, Studies of β-delayed proton decays of N $\approx$ Z nuclei around ^{100}Sn at the GSI-ISOL facility, Nucl. Phys. A **746**, 66 (2004).

[50] O. Kavatsyuk, M. Kavatsyuk, L. Batist, A. Banu, F. Becker, A. Blazhev, W. Brüchle, J. Döring, T. Faestermann, M. Górska, H. Grawe, Z. Janas, A. Jungclaus, M. Karny, R. Kirchner, M. La Commara, S. Mandal, C. Mazzocchi, I. Mukha, S. Muralithar *et al.*, Beta decay of ^{103}Sn, Eur. Phys. J. A **25**, 211 (2005).

[51] R. D. Page, P. J. Woods, R. A. Cunningham, T. Davinson, N. J. Davis, A. N. James, K. Livingston, P. J. Sellin, and A. C. Shotter, Decays of odd-odd $N - Z = 2$ nuclei above ^{100}Sn: The observation of proton radioactivity from ^{112}Cs, Phys. Rev. Lett. **72**, 1798 (1994).

[52] P. T. Wady, J. F. Smith, E. S. Paul, B. Hadinia, C. J. Chiara, M. P. Carpenter, C. N. Davids, A. N. Deacon, S. J. Freeman, A. N. Grint, R. V. F. Janssens, B. P. Kay, T. Lauritsen, C. J. Lister, B. M. McGuirk, M. Petri, A. P. Robinson, D. Seweryniak, D. Steppenbeck, and S. Zhu, γ-ray spectroscopy of the odd-odd $N = Z + 2$ deformed proton emitter ^{112}Cs, Phys. Rev. C **85**, 034329 (2012).

[53] D. Schardt, R. Kirchner, O. Klepper, W. Reisdorf, E. Roeckl, P. Tidemand-Petersson, G. Ewan, E. Hagberg, B. Jonson, S. Mattsson, and G. Nyman, Alpha decay studies of tellurium, iodine, xenon and cesium isotopes, Nucl. Phys. A **326**, 65 (1979).

[54] F. Heine, T. Faestermann, A. Gillitzer, J. Homolka, M. Köpf, and W. Wagner, Proton and alpha radioactivity of very neutron deficient Te, I, Xe and Cs isotopes, studied after electrostatic separation, Z. Phys. A: Hadrons Nucl. **340**, 225 (1991).

[55] L. Capponi, J. F. Smith, P. Ruotsalainen, C. Scholey, P. Rahkila, L. Bianco, A. J. Boston, H. C. Boston, D. M. Cullen, X. Derkx, M. C. Drummond, T. Grahn, P. T. Greenlees, L. Grocutt, B. Hadinia, U. Jakobsson, D. T. Joss, R. Julin, S. Juutinen, M. Labiche *et al.*, Delayed or absent $\pi(h_{11/2})^2$ alignment in ^{111}Xe, Phys. Rev. C **101**, 014313 (2020).

[56] D. Schardt, T. Batsch, R. Kirchner, O. Klepper, W. Kurcewicz, E. Roeckl, and P. Tidemand-Petersson, Alpha decay of neutron-deficient isotopes with $52 \leqslant Z \leqslant 55$, including the new isotopes ^{106}Te ($T_{1/2} = 60_{\mu s}$) and ^{110}Xe, Nucl. Phys. A **368**, 153 (1981).

[57] M. Wang, G. Audi, A. Wapstra, F. Kondev, M. MacCormick, X. Xu, and B. Pfeiffer, The Ame2012 atomic mass evaluation, Chin. Phys. C **36**, 1603 (2012).